Zeitschrift: Orion : Zeitschrift der Schweizerischen Astronomischen Gesellschaft
Herausgeber: Schweizerische Astronomische Gesellschaft
Band: 63 (2005)
Heft: 326

Artikel: Aspects of Geneva photometry : part 3 : doing physics with colours
Autor: Cramer, Noël
DOI: https://doi.org/10.5169/seals-897735

Aspects of Geneva Photometry[1]

Part 3 - Doing Physics with Colours

NOËL CRAMER

In this third part of the article, we consider the manner in which the multicolour photometric measurement can be calibrated in terms of primary data that, taken as a first example, is not sensitive to interstellar reddening. We consider the MK spectral classification as well as effective temperatures and bolometric corrections for the B-type stars. We also describe a good correlation between Geneva photometry and the STRÖMGREN photometric Hβ index, leading to what we may call a «hyperindex» sensitive to emission in the Hβ line. Some unsuspected inconsistencies are revealed and briefly discussed.

5. The colours of basic Stellar Physics

5.1 Preliminary remarks

We have seen in Part 2 that the accurate measurement of starlight with the aid of distinct «coloured» filters of precisely defined passbands, distributed over the spectral range where our atmosphere is transparent to the shorter wavelengths (the «visible» spectral range), can lead to a classification of stars in terms of temperature and, within certain limits, of surface gravity. Actually, if we set aside interstellar extinction, this «colorimetric» analysis of starlight is also sensitive to variations of abundance of the small amounts of elements heavier than Helium (called «metals» by astronomers) that are present in stellar atmospheres. The colours are also affected by unresolved companion stars, or by the rotational velocity of the star as well as by other intrinsic physical peculiarities. All these factors complicate the interpretation of multicolour photometry and we shall discuss them later on.

The colorimetric information provided by multicolour photometry basically relates to the «surface» physical properties of stars. On the other hand, the precise measurement of photometric variability in time provides further information regarding their internal constitution, and the extreme accuracy (millimagnitude to nanomagnitude) required by «asteroseismology», when feasible, provides the most powerful tool for that purpose. Stellar variability is a whole subject by itself, and we shall restrict this discussion to stellar classification by «colours».

The following physical quantities are best perceived by multicolour photometry:

- As mentioned in Part 2, the effective temperature T_{eff} is a first order effect. If F is the electromagnetic flux (erg s^{-1} cm^{-2}) emitted by the star *at its surface*, the «effective temperature» T_{eff} is defined by convention in terms of the STEFAN-BOLTZMANN radiation law by $F = \sigma(T_{eff})^4$
- In a less direct manner, surface gravity $g = GM/R^2$ (cm s^{-2}) may also be estimated. Astronomers are accustomed to using its logarithmic expression.
- The absolute magnitude, for instance in the V passband M_v, is well correlated to colour via the relation of stellar luminosity to temperature and surface gravity. The absolute magnitude M_v is by convention the apparent magnitude in the V band, m_v, of the star seen at a distance of 10 parsecs (1 parsec = 3.2616 light-years = 206265 AU = 3.0857 10^{18} cm) in absence of interstellar extinction.
- The fact that the stellar flux is sampled in a restricted spectral region (V passband) requires the further knowledge of the related bolometric correction B.C.. This is the correction to M_v necessary to obtain the total absolute (bolometric) magnitude integrated over the whole spectrum, $M_{bol} = M_v + B.C.$. This value is important for evaluating the stellar luminosity L (total radiation energy output per unit time), a basic parameter in theoretical stellar modelling as it expresses the «power» generated by the thermonuclear reactions in the star's core. L is generally referred to the solar value $L\odot = 3.85\ 10^{26}$ W. Knowing that for the sun $M_{bol}\odot = 4.74$ mag, we easily derive the following relation: $M_{bol} = 4.74 - 2.5 \log(L/L\odot)$, thus defining L. And, in a wider scope, we have $L = 4\pi R^2\sigma(T_{eff})^4$, which links the above mentioned quantities.

The intrinsic colours, i.e. the true stellar colour indices in the absence of interstellar extinction, must be known if we are to use them to derive the quantities mentioned above. In a sense, the three X,Y,Z parameters are already «intrinsic» *colour combinations* reflecting the properties of the stellar spectral energy distributions corrected for interstellar reddening. But, if we are to make use of fundamental data that are obtainable only by other means, such as stellar parallaxes (= geometrical distances), we must be able to estimate the extinction by interstellar dust in, say, the V filter to be able to derive the

Fig. 35. Accurate multicolour photometry needs perfect atmospheric transparency, such as that encountered at 3600m at the Jungfraujoch Sphinx Observatory.

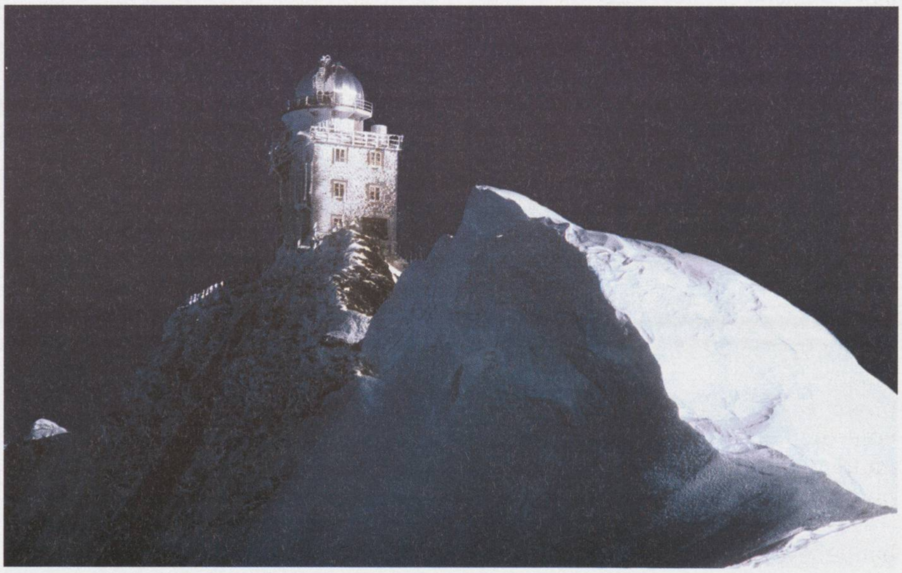

[1] Adapted from Archs Sci. Genève, Vol. 56, Fasc. 1, pp. 11-38, Juillet 2003. Based on data acquired at the La Silla (ESO, Chile), Jungfraujoch and Gornergrat (HFSJG International Foundation, Switzerland), and Haute-Provence (OHP, France) observatories.

corresponding absolute magnitudes M_V. We will see later that the quest for intrinsic colours is central to the study of B-type stars via calibrations established empirically for multicolour photometry.

5.2. Calibrating photometry

As referred to above, photometric calibrations are essentially achieved by correlating in an optimum manner the observable photometric quantities with particular physical quantities that have been securely determined otherwise by the most appropriate observational techniques. The latter are, however, as a rule laborious and limited to a small number of nearby stars (e.g. trigonometric parallaxes, or the measurement of stellar apparent angular diameters, etc.). The object of a photometric calibration is to extend, by correlation analysis, the volume of space that can be studied on the basis of those fundamental data to much greater distances.

The search of that «optimum» correlation is the most important initial step of the process. Quite generally, the strategy of the analysis will depend on the properties of the system – i.e. the way its different passbands sample the energy distribution – and on the quantity to be estimated. Optimisation includes the search for *simplicity*, which is ideally also that of the minimal set of assumptions – or parsimony – regarding the basic calibration data. Thus, one should give greatest weight to «primary» physical data, whereas data of the same nature but derived via a more elaborate series of processes which may be laden with biases should be given less weight, if not discarded altogether. Even primary data do, however, «evolve» with time as instrumental techniques get better – e.g. trigonometric parallaxes which have gained hugely in accuracy since the Hipparcos Astrometric Satellite concluded its mission in 1997, or pending the forthcoming application of large interferometric telescope complexes to determine fundamental parameters such as stellar angular diameters – and some types of calibrations will consequently stay more «robust» than others depending on the quality of the primary data.

One must now mention the advent during these last three decades of sophisticated theoretical stellar atmosphere models which have decisively contributed to the interpretation of multicolour photometry. «Synthetic photometry» done by filtering realistic theoretical fluxes through sets of passbands would, ideally, link the basic physical quantities (temperature, surface gravity, chemical composition, etc.) of the models with the observed fluxes, help us to choose the most appropriate colour-colour representation and allow us to determine the regions where it performs best, thus also revealing the best shape of a possible calibration relation. However, the present state of the art does not enable a reliable calibration to be achieved independently, because synthetic photometry is heavily burdened by assumptions affecting the models as well as by uncertainties regarding the true shapes of the passbands. An example of such a synthetic «calibration» of the X, Y parameters in terms of effective temperature and surface gravity for the most massive stars by means of solar composition models computed by KURUCZ (1993) is given in fig 36. It is immediately apparent that the theoretical colours do not perfectly fit the sequence of the «real» stars. However, even if the zero points and scales are not perfectly accurate, the general shape of such a relation is presumably true, and empirical – i.e. minimally assuming – fundamental data can be profitably used to adjust it in most cases (see for example KÜNZLI et al 1997, or later on in this article). The models are also very useful to point out the existence of regions of photometric ambiguity such as for the temperatures lower than 10000 K at Y ≈ -0.2, in fig 36, where one-to-one correlations are evidently unfeasible in this particular parameter space.

Therefore, and for all practical purposes, the calibrations of the X, Y diagram are restricted to values of Y ≥ -0.06 and to gravities higher than log g ≈ 3 (see Fig 36). The Z parameter equally serves to discriminate against the cool Mira-type variables (see Fig 34, [Part 2]) by restricting its validity to Z ≤ 0.03.

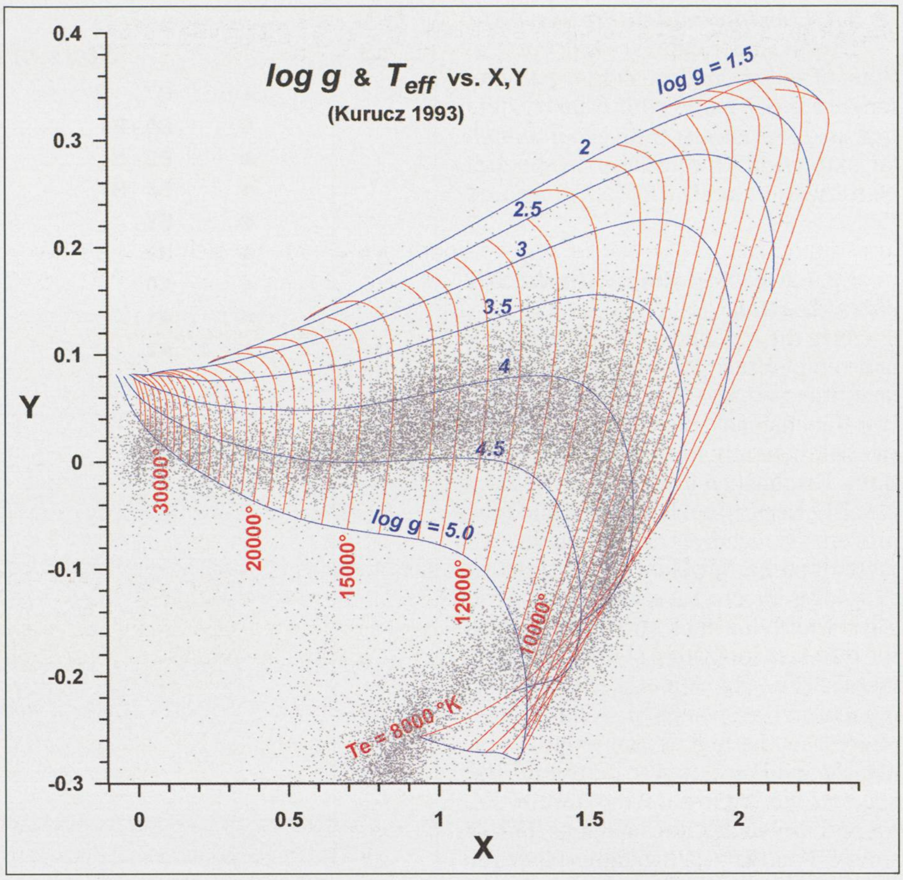

Fig. 36. The T_{eff} vs. log g grid of the stellar atmosphere models with solar composition computed by KURUCZ (1993), overlaid on the observed locations of the O, B, A and first F-type stars in the X, Y parameter diagram. One notes that the overlap is far from perfect although the theoretical relation would reproduce the general shape of the observed distribution better if it were somewhat distorted. The models do, however, reveal a region of ambiguity between 8000 K and 10000 K where the effects of temperature and surface gravity tend to cross over. They also show that photometry loses much of its sensitivity at higher temperatures. There is also some ambiguity at the upper envelope (lower gravities) where we find the brightest supergiants and where the lines of equal temperature curve to the left. The grid of models shown in this figure was cut off at 8000 K.

5.2.1. Using reddening-free data

The most straightforward correlations of reddening-free colour parameters are those made with primary data that are likewise insensitive to interstellar extinction. One of these is spectral classification and will be presented first.

5.2.1.1. Correlating with the MK classification

As in the X, Y plane of Fig 36, gravity and temperature are also the physical quantities at the basis of the YERKES MKK two-dimensional spectral classification (more frequently named MK classification). Established in 1943 by W.W. MORGAN, P.C. KEENAN and E. KELLMAN and now universally used as an adequate estimate of stellar physical characteristics (T_{eff}, log g, M_V, etc.), it is based on the relative widths of lines corresponding to the different ionization states of various metals (Fe, Mg, Mn, Ca, Si, H, etc.) present in the spectra of stellar atmospheres. At the higher temperatures Si, Mg, He and H are used to determine the *spectral type*. At lower temperatures Fe, Ca and molecular lines such as TiO or even CH and ZrO gain in importance for the same purpose. The second dimension, the *luminosity class*, is estimated by the line widths (less gravity → less pressure → narrower lines), as mentioned earlier regarding the Y parameter in Part 2. However, the level of ionization of a gas depends essentially on temperature but also does so to a lesser degree on pressure. The numerical ratio of two consecutive ions of a same element is the result of the equilibrium between *ionization* (by radiation and collisions) and *recombination* (collision of ions with electrons) processes. The MK classification criteria rely on such ratios. At the reduced pressure of the extended atmospheres of giants and supergiants, the recombination to ionization ratio tends to decrease (lower probability for electron – ion collisions, thus reducing recombination). So, when the specific classification criteria of the MK system are applied, giants and supergiants tend to have lower effective temperatures

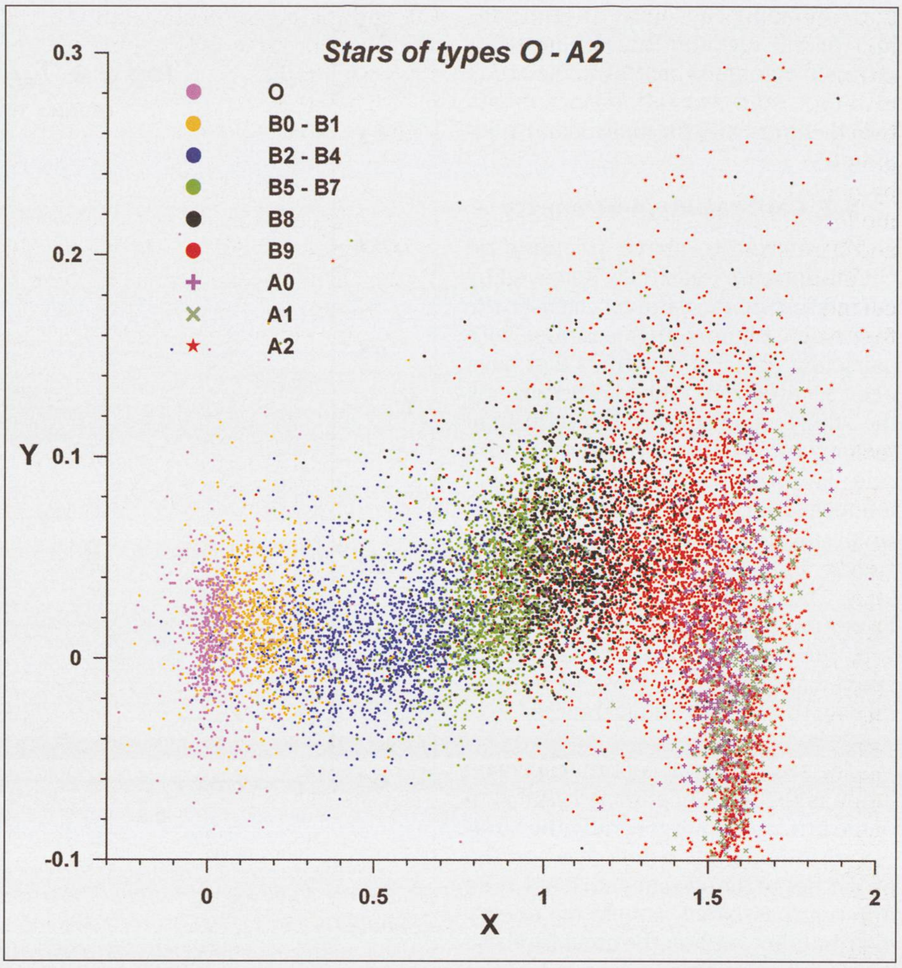

Fig. 37. The stars of MK spectral types O to A2 in the X, Y diagram. Photometry separates temperature essentially in the same manner as spectral classification. The O stars show a small residual effect of reddening (which in this diagram shifts them blue-ward!) due to extreme values of interstellar extinction.

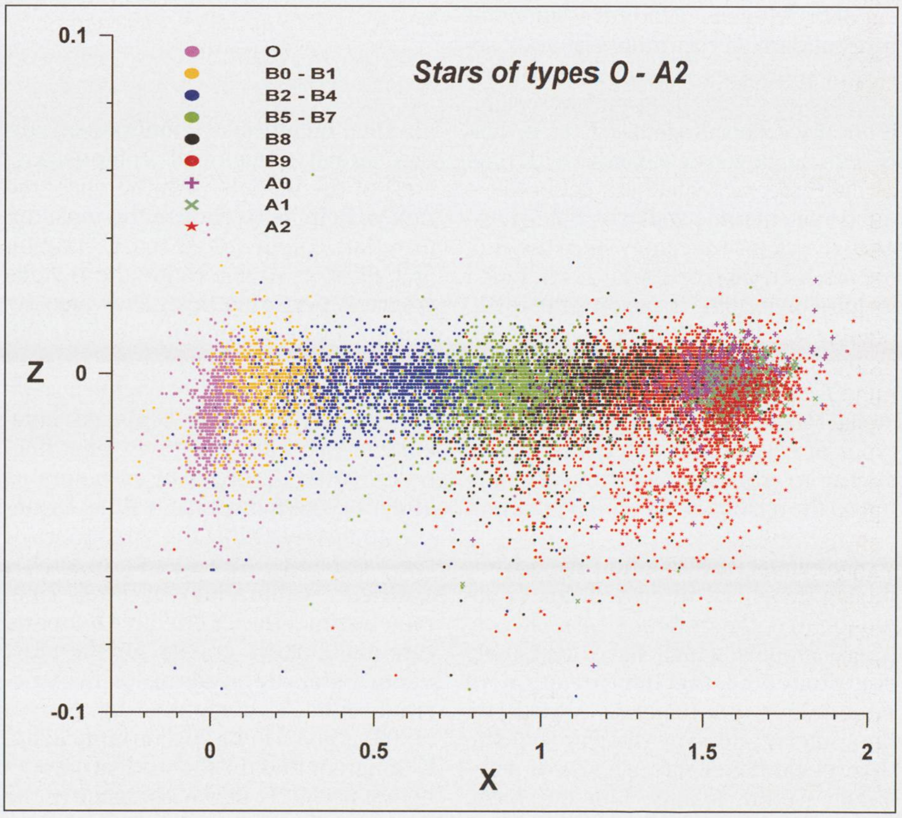

Fig. 38. The same stars as in Fig 37, but in the X, Z diagram. The extended scale of the Z axis shows the extreme narrowness of the sequence. The X parameter is a good spectral type (i.e. temperature) estimator between types O to A0. The A1 and A2 stars begin to detach themselves from the rectilinear sequence as seen in the broader scope of Fig 33, (Part 2). A residual effect due to extreme interstellar extinction is apparent for the O stars, as in Fig 37.

than the main sequence «dwarfs» (i.e. non-evolved class V stars) at a given spectral type. The situation is, however, reversed in the A0 to G0 interval due to the classification criteria used in that region. These circumstances are reflected by photometry in the behaviour of the models and correlations in figures 36 and 40 as also 32 (Part 2).

The distribution of the MK sub-classes and luminosity classes of O, B and first A-type stars is shown in Figs 37 to 39, and the mean locations of the MK types in the same colour diagram are shown in Fig 40.

This correlation was originally presented by CRAMER (1994). A slightly improved version of the latter is presented here, and is listed in Table 1.

The calibration is based on about 4000 stars, some 80% of which have MK types taken from the various editions of the Michigan Catalogue (HOUK et al. 1975 and subsequent volumes). The poor discrimination among O-B1 stars as well as the above-mentioned regions of ambiguity are apparent in fig 40. One also notices the region of ambiguity regarding MK type, as seen in Fig 39, for B5 to B7 stars of classes V and III. NANCY HOUK has pointed out (private communication, see CRAMER 1994) that this does indeed correspond to a difficulty in the spectral classification procedure. The error bars in the figure reflect the dispersion ($\sigma N^{-1/2}$) of each correlation in

Table 1: MK type versus X,Y,Z relation

Class V	X	Y	Class IV	X	Y	Class III	X	Y	Class II	X	Y
O6	-0.009	0.010	O9IV	-0.001	0.010	O9III	0.022	0.015	O9II	0.017	0.014
O7	-0.006	0.011	O9.5IV	0.055	0.011	O9.5III	0.040	0.016	O9.5II	0.020	0.015
O8	-0.003	0.012	B0IV	0.092	0.012	B0III	0.044	0.017	B0II	0.045	0.016
O9V	0.034	0.015	B0.5IV	0.137	0.012	B0.5III	0.126	0.022	B0.5II	0.108	0.018
O9.5V	0.072	0.018	B1IV	0.229	0.011	B1III	0.201	0.022	B1II	0.154	0.020
B0V	0.103	0.020	B1.5IV	0.280	0.010	B1.5III	0.284	0.021	B1.5II	0.220	0.022
B0.5V	0.193	0.018	B2IV	0.356	0.010	B2III	0.324	0.020	B2II	0.253	0.023
B1V	0.260	0.015	B2.5IV	0.520	0.011	B3III	0.598	0.019	B3II	0.377	0.025
B1.5V	0.324	0.010	B3IV	0.656	0.017	B4III	0.694	0.019	B4II	0.580	0.037
B2V	0.468	0.002	B4IV	0.710	0.020	B5III	0.837	0.032	B5II	0.723	0.045
B2.5V	0.546	-0.001	B5IV	0.750	0.025	B6III	0.912	0.042	B7II	0.880	0.054
B3V	0.609	0.000	B6IV	0.899	0.040	B7III	0.941	0.048	B8II	0.942	0.060
B4V	0.689	0.001	B7IV	0.959	0.048	B8III	1.057	0.068	B9II	1.004	0.070
B5V	0.756	0.005	B8IV	1.062	0.056	B9III	1.265	0.093	A0II	1.685	0.259
B6V	0.878	0.015	B9IV	1.315	0.065	B9.5III	1.375	0.100	A5II	2.161	0.267
B7V	0.930	0.020	B9.5IV	1.480	0.054	A0III	1.550	0.095	A7II	2.031	0.142
B8V	1.129	0.044	A0IV	1.565	0.036	A1III	1.663	0.043			
B8.5V	1.217	0.050	A1IV	1.640	-0.026	A2III	1.653	-0.025			
B9V	1.404	0.046	A2IV	1.621	-0.066	A3III	1.612	-0.074			
B9.5V	1.493	0.034	A3IV	1.600	-0.113	A5III	1.532	-0.107			
A0V	1.557	0.011									
A1V	1.595	-0.017									
A2V	1.615	-0.049									
A3V	1.609	-0.071									

Class Ia	X	Y	Class Iab	X	Y	Class Ib	X	Y
B0Ia	0.017	0.015	B0Iab	0.020	0.015	B0Ib	0.058	0.020
B0.5Ia	0.053	0.017	B0.5Iab	0.039	0.017	B0.5Ib	0.082	0.021
B1Ia	0.058	0.018	B1Iab	0.132	0.023	B1Ib	0.140	0.024
B1.5Ia	0.128	0.023	B2Iab	0.271	0.035	B1.5Ib	0.196	0.030
B2Ia	0.160	0.030	B3Iab	0.387	0.050	B2Ib	0.260	0.039
B2.5Ia	0.220	0.035	B5Iab	0.530	0.068	B2.5Ib	0.320	0.043
B3Ia	0.300	0.047	B6Iab	0.620	0.081	B3Ib	0.465	0.050
B4Ia	0.340	0.055	B7Iab	0.743	0.100	B5Ib	0.600	0.065
B5Ia	0.397	0.065	B8Iab	0.830	0.120	B6Ib	0.670	0.072
B6Ia	0.480	0.083	B9Iab	0.926	0.140	B7Ib	0.810	0.090
B8Ia	0.530	0.095	A0Iab	1.080	0.170	B8Ib	0.890	0.100
B9Ia	0.666	0.120	A2Iab	1.370	0.240	B9Ib	1.100	0.145
A0Ia	0.810	0.150	A3Iab	1.550	0.280	A0Ib	1.434	0.229
A1Ia	0.980	0.180	A7Iab	1.805	0.290	A1Ib	1.650	0.280
A2Ia	1.200	0.225	F0ab	2.100	0.260	A2Ib	1.720	0.290
A3Ia	1.429	0.270	F2Iab	2.150	0.190	A3Ib	1.900	0.300
A5Ia	1.650	0.300	F3Iab	2.100	0.104	A4Ib	2.080	0.290
F0Ia	1.787	0.302	F5Iab	1.599	-0.108	A5Ib	2.106	0.270
F2Ia	1.889	0.250				A7Ib	2.090	0.232
F5Ia	1.795	0.200				F0Ib	2.055	0.145

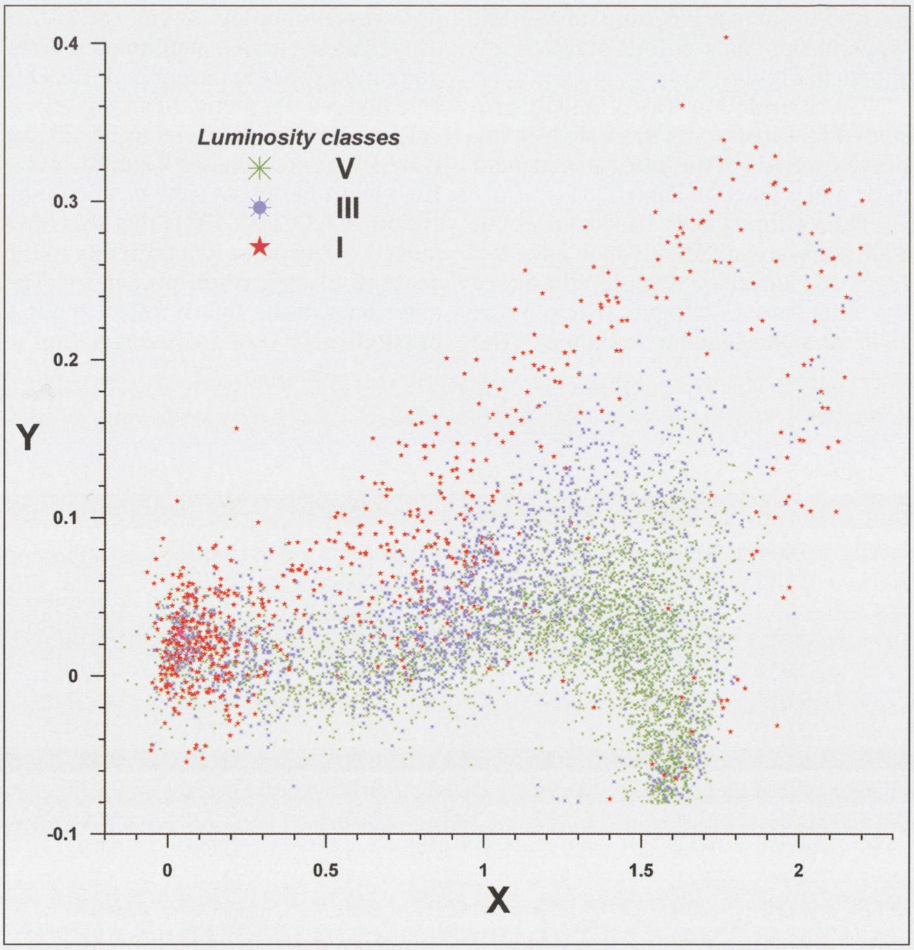

Fig. 39. The separation of luminosity classes in the same representation as in Figs 37 and 38. The apparent overlap of part of the class III stars with class V in the region 0.65 < X < 1.15 coincides with a known difficulty of the luminosity class determination for B5 to B7 stars in the MK system (See remark by NANCY HOUK in the discussion following CRAMER [1994]).

the extreme cases of the class V and Ia sequences, and have been included here for the purpose of illustration.

A question arises regarding the relevance of such a calibration. This question has been asked the author at several occasions, notably by spectroscopists. The first part of an answer lies in the fact that a good correlation between photometry, which is exclusively quantitative, and spectral classification, which relies somewhat more on the judgment of the person doing the classification, is feasible. This helps both communities to «speak the same language» regarding physical parameters. Another, and important, aspect is that a good calibration in terms of a homogeneous photometric system not only allows the two partners of the initial correlation to agree with each-other, but also enables us to examine, via the photometric homogeneity, the consistency of other sources of spectroscopic data. In other words, the reliability of MK types derived by various authors may be directly compared even if their samples of stars do not overlap, provided photometry is available for all the data. It is known, but not often stated, that significant systematic differences sometimes exist between the classifications done by different authors, even though the same MK standard spectral sequence is presumably used.

5.2.1.2. Effective temperature and bolometric correction

As seen in fig 26, (Part 2), effective temperature is one of the first order effects of multicolour photometry due to its colorimetric nature. It is also a fundamental quantity serving to link observations with theoretical modelling of stellar atmospheres and internal structure. The literature regarding calibrations, either photometric or spectroscopic, and

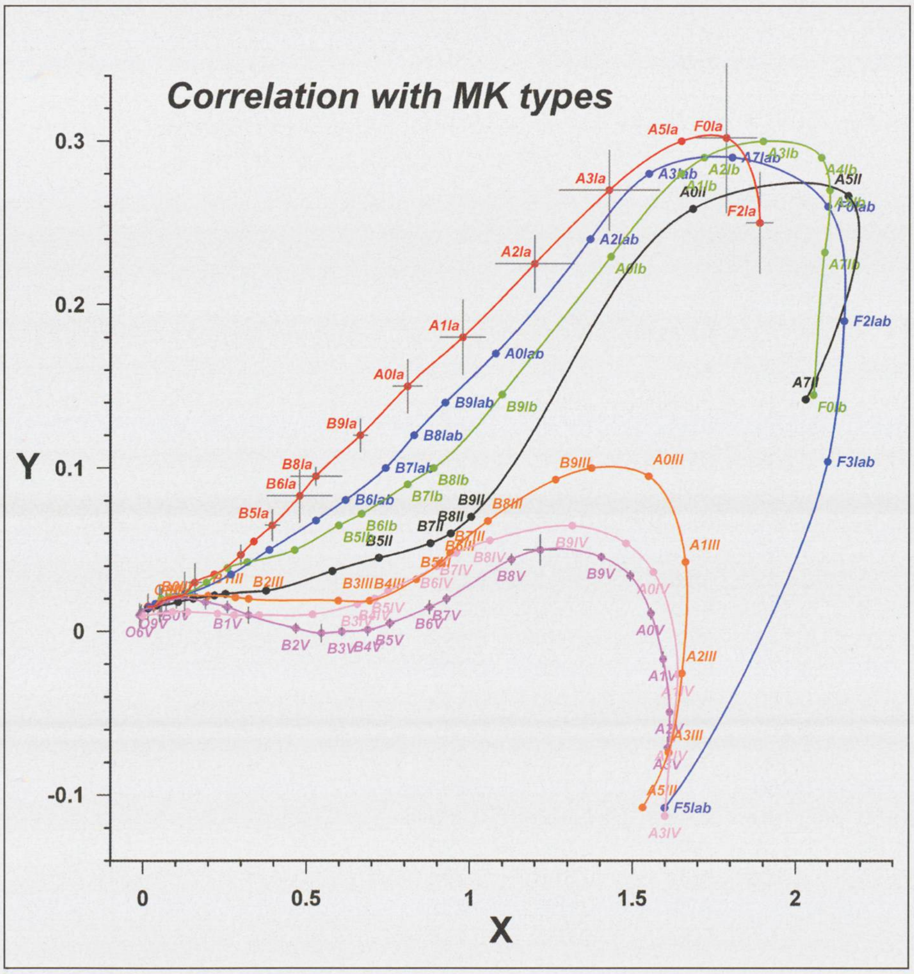

Fig. 40. The mean locations of the MK spectral types and luminosity classes. The correlation is based on 4000 stars. The dispersions around the mean are shown here for the extreme cases of the classes V and Ia. Note the small dispersions of the much more numerous class V samples.

their resulting estimates of T_{eff} is extensive. Fundamental empirical data of that sort are, however, still not very common for the most massive stars due to technical reasons involving angular resolution and bolometric (whole electromagnetic spectrum) flux measurement.

This is particularly true for the hot and massive O and B-type stars. They are globally more distant than the relatively much more numerous cooler types and the apparent angular diameters of the closest ones are very small – of the order of 10^{-3} seconds of arc. Their radiated fluxes shortward of the atmospheric cut-off ($\lambda \approx 3000$ Å) are relatively important due to their high temperatures and necessitate space-based measurements to reliably cover the whole spectrum. For example, an A0 star radiates almost half of its energy shortward of 3000 Å, whereas for an O star that value is closer to 95%.

As seen above, we have the total stellar luminosity $L = 4\pi R^2 F$. And at the distance d we have the observed flux density f:

$$f = L / 4\pi d^2 = (R^2 / d^2)F = (\alpha / 2)^2 \sigma (T_{eff})^4$$

Where $\alpha = 2R/d$ is the observed angular diameter of the star. The effective temperature T_{eff} is thus defined if f and α can be measured. The bolometric correction B.C., on the other hand, is only a ratio requiring the knowledge of the star's entire radiated spectral energy distribution and the transmission function of the passband that is to be «corrected».

One has to go back to the original interferometric work of CODE et al (1976) for the most direct estimate of T_{eff} of a few nearby stars obtained with the 188m baseline Narrabri intensity interferometer in Australia. The absolute flux distributions were measured by the OAO-2 satellite for the ultraviolet, and by ground-based spectro-photometry for the rest of the spectrum. The interferometrically determined angular diameters had to be corrected for limb darkening affecting the stellar apparent disks. The interstellar extinction of the flux distributions had to be de-reddened. Corrections had to be made for a number of stars members of binary systems. So, these empirical T_{eff} and B.C. are not totally model-independent. But the work was done as carefully as possible, and we will have to wait until modern interferometers such as the VLTI significantly improve their accuracy and

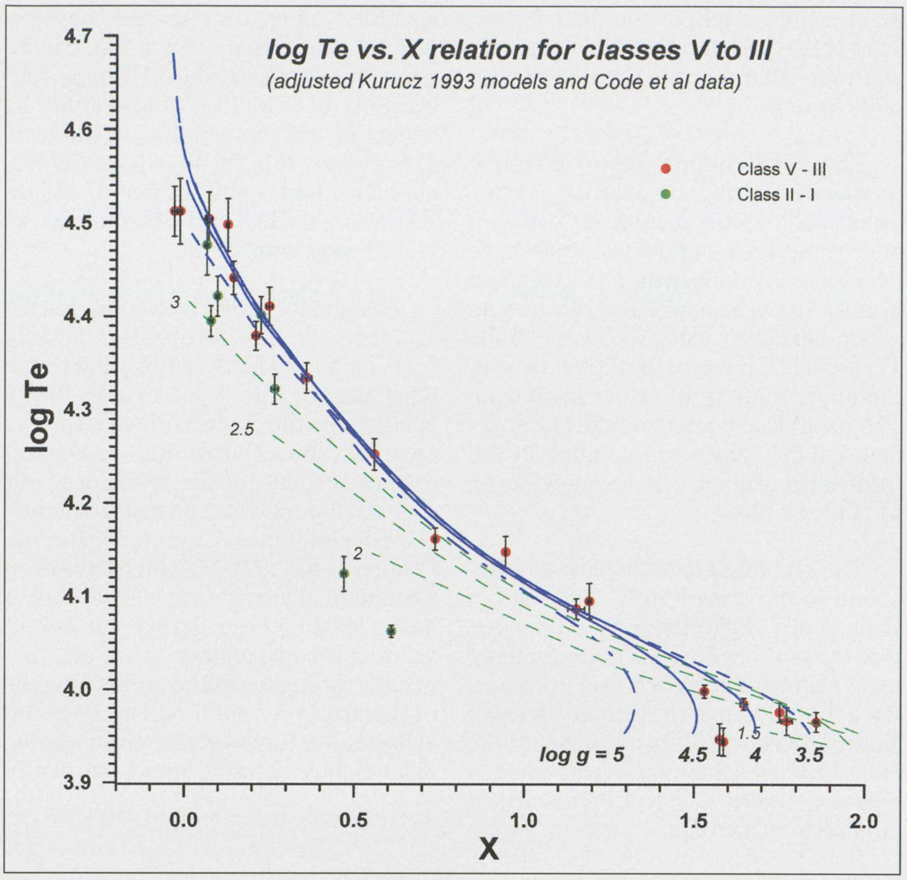

Fig. 41. Kurucz's (1993) models adjusted to fit a log T_{eff} versus X relation through the empirical data of Code et al. for O, B and first A stars of classes V to III. The lines of lower gravity as well as the bright giants and supergiants have been included for comparison.

Fig. 42. Synthetic relations for the bolometric correction adjusted to those of Code et al. Same comments as for fig 40.

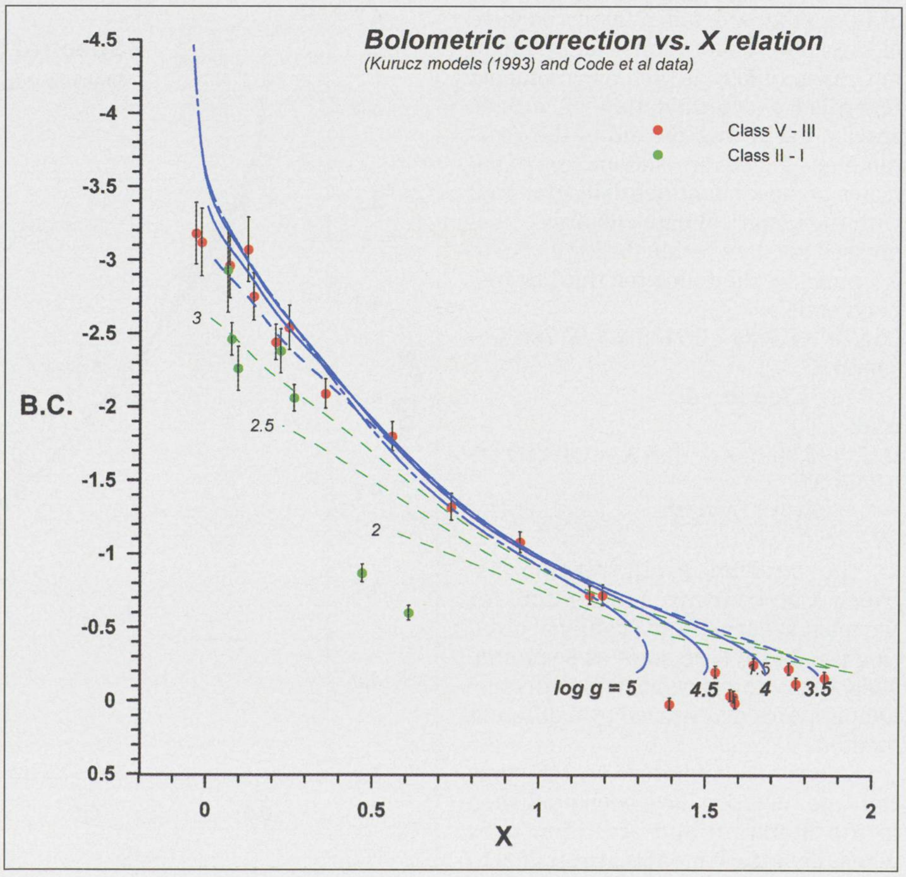

extend the sample in the near future. That is the reason why we have included these calibrations in this sub-section of the article.

Empirical calibrations of effective temperatures and bolometric corrections based on the results of CODE et al and using the X parameter alone have been presented elsewhere (CRAMER and MAEDER 1979; CRAMER 1984a). We may go a step further by using the *shape* of the T_{eff} versus X relation predicted by synthetic photometry to fit the same data. The result is expected to take better account of the «physics» that underlie the form of the sequence and is shown in fig 41 (CRAMER 1999).

The empirical data displayed correspond to the class V to III O-B stars of CODE et al's (1976) list, where the stars that the authors corrected for duplicity have also been adjusted here to reproduce the colours of the primary. A small shift (0.035 mag) of the X values of the (KURUCZ 1993) solar models was made to optimise the fit and will be discussed later on in this article.

The bolometric correction computed by KURUCZ is adjusted in the same manner, and the corresponding bolometric corrections of the models are given in fig 42.

They also agree perfectly with those of CODE et al. A detailed tabulated form of these two calibrations can be found in CRAMER (1999) as well as comments regarding a determination of surface gravity, log g, with the aid of the Y parameter. However, satisfactory estimates of these quantities that agree well with the empirical data can also be expressed for stars within the log g = 3.5 to 4.5 range by the following third degree polynomials:

$$\text{Log Te} = 4.5424 - 0.7138\,X + 0.3785\,X^2 - 0.0894\,X^3$$
for log Te ≥ 4

And

$$\text{B.C.} = -3.3501 + 3.6156\,X - 1.4928\,X^2 + 0.2551\,X^3$$
for B.C. ≤ -0.02

The straightforward relation between X and effective temperature for the main sequence and slightly evolved (log g ≈ 3.5) B-type stars as seen here calls for a comparison with effective temperatures determined by a different method.

Effective temperature vs. MK spectral type relations have been published in the literature and are often used when theoretical models are applied to specific studies in stellar astrophysics. A quite instructive comparison can be made here with standard MK-type calibrations of effective temperature by using the MK correlation of Table 1. This is shown in fig 43, where the frequently cited calibrations of BÖHM-VITENSE (1981) and SCHMIDT-KALER (1982) were considered.

In spite of the 5% errors reported for T_{eff}, the sequences diverge significantly for 0.4 < X < 0.7 (B2V to B5V) and somewhat also for 0.9 < X < 1.1 (B7V – B8V). Neither do the uncertainties over the mean X values (horizontal error bars) help to account for the deviations. Our spectral type correlation rests essentially on the MK-types of the Michigan catalogue (HOUK et al 1975) which have been systematically used in the Geneva data base. Maybe these deviations reflect some of the dispersion, or biasing, that occurs throughout the various sources of spectral types published in the general literature. However, this troublesome discrepancy certainly tends to justify the «relevance» of correlating a homogeneous photometry with the MK spectral classification, as discussed above.

5.2.1.3. Correlation with the Strömgren reddening-free Hβ index

The correlation of the X,Y parameters with the STRÖMGREN Hβ index is particularly interesting because of the extremely different natures of the two photometries. The X,Y parameters essentially reflect the behaviour of the continuum over the visible spectral range, whereas the β index specifically measures the strength of the Hβ line by means of a narrow and wider band, both centred on the line. Moreover, the Geneva passbands only marginally include that line (See Fig. 1, (Part 1)). An excellent correlation for normal stars was obtained (CRAMER 1984b) and is expressed by the β(X,Y) polynomial estimator.

The relation, defined for O, B and first A type stars of classes V to III, does nevertheless extrapolate correctly to bright giants and supergiants, as far as has been verified for a few dozen cases.

Fig. 43 The relation of fig 41 compared with the MK type versus T_{eff} calibrations of BÖHM-VITENSE (1981) and SCHMIDT-KALER (1982). The X value is determined by our MK type calibration. The vertical error bars are the estimated 5% errors on T_{eff} and the horizontal ones the dispersion in X.

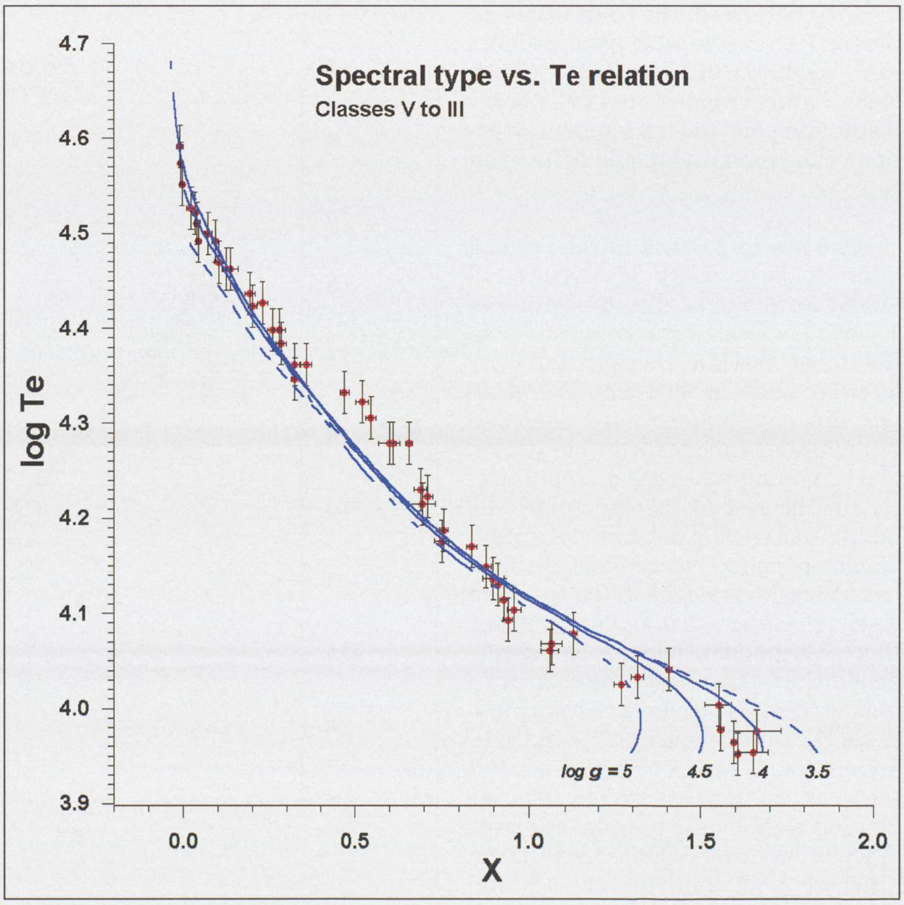

$$\beta(X,Y) = a_0 + a_1X + a_2Y + a_3XY + a_4X^2 + a_5Y^2 + a_6XY^2 + a_7X^2Y + a_8X^3 + a_9Y^3$$

where:

a_0	a_1	a_2	a_3	a_4	a_5	a_6	a_7	a_8	a_9
2.5909	0.0667	-0.6801	-0.2559	0.1748	-2.4676	0.1448	0.2582	-0.0612	0.4418

The details of the calibration are discussed in the original paper. It is mapped into the X,Y plane of fig 44 which also contains almost 12800 stars as a background within the validity range. The standard deviation over the residuals for the 950 calibration stars is only 0.016 mag.

Such a good correlation encourages us to form what we may call a «*hyperindex*», i.e. an index composed of quantities issuing from two different photometric systems. Here, we consider the $\delta\beta = [\beta(X,Y) - \beta]$ «*hyperindex*». Due to the specific nature of the β index, δβ is very sensitive to any departures from the norm that may occur in the Hβ line. That is particularly evident in the case of emission in the hydrogen lines and makes δβ a powerful detector of Be stars in their emission phase. The X,Y parameters are indeed virtually unaffected for moderate emission, and much less so than β when strong hydrogen emission lines are present.

Fig.45 (taken from CRAMER 1984b) shows the large amplitude of the variation for Be stars and its dependence on temperature and projected rotational velocity. High rotational velocity tends to generate an equatorial disk of gas that fluoresces under the intense ultraviolet radiation of the parent star. In the same paper, it was suggested that rotation was less susceptible to affect the true β index than was formerly believed; this was later confirmed by GARRISON and GRAY (1991). The δβ index was also shown to have the capacity of estimating the *equivalent width of the emission feature in Hβ*; a feat usually achieved only by medium- to high resolution spectroscopy. The differential equivalent width estimator of the emission feature is $\delta W \cong 34\,\delta\beta$ in Å units.

In this context, we may quote C. JASCHEK (1987, p. 94) on peculiar spectral lines and photometry: «*The situation changes if spectral peculiarities are considered. Here the spectroscopists have the advantage; they can quickly recognize a large number of peculiarities, whereas photometrists are more or less helpless. Consider just one case: the Hβ measurements which are central for luminosity determinations of early type stars. Since photometrists measure an equivalent width, but do not see the profiles, they cannot know if a star is a supergiant with intrinsi-*

Fig. 44 The β(X, Y) relation overlaid with 12800 stars within its validity range.

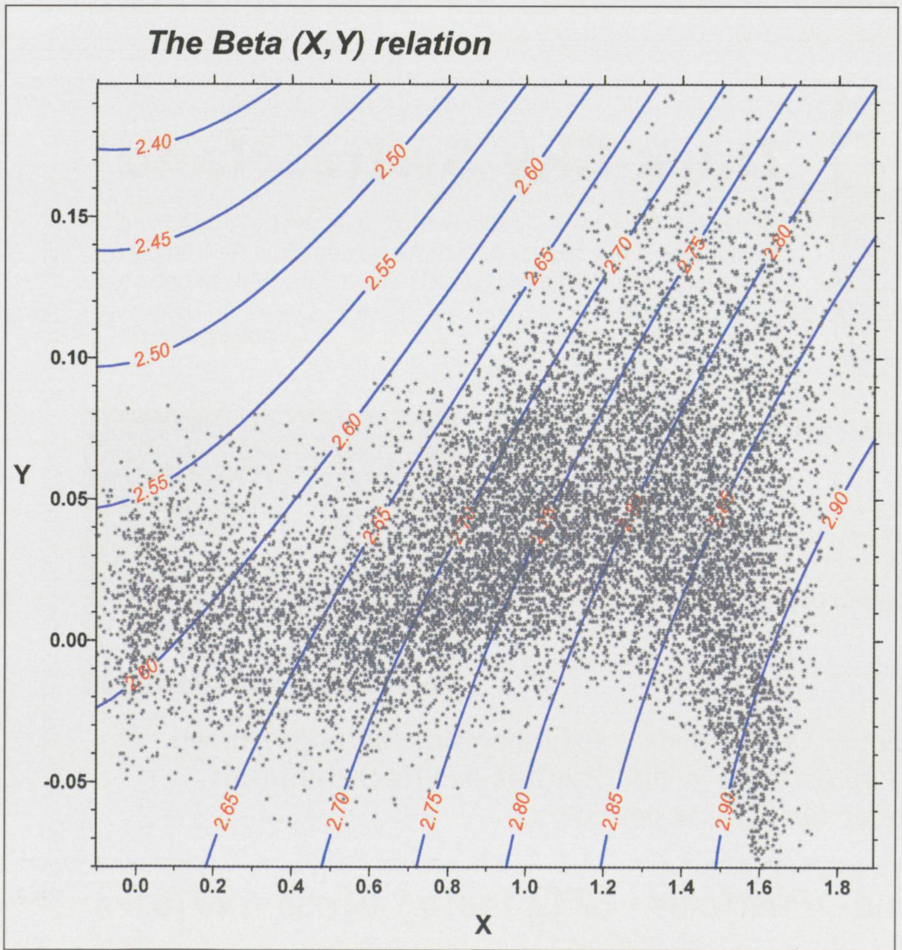

Bibliography 3

BÖHM-VITENSE, E.:1981, *The effective temperature scale*, in Ann. Rev. Astron. Astrophys. 19, 295

CODE, A.D., DAVIS, J., BLESS, R.C., HANBURY BROWN, R.: 1976, *Empirical effective temperatures and bolometric corrections for early-type stars*, ApJ. 203, 417

CRAMER, N., MAEDER, A.:1979, *Luminosity and T_{eff} determinations for B-type stars*, A&A 78,305

CRAMER, N.: 1994, *The MK Classification of B-Type Stars as seen by Geneva Photometry*, in The MK Process at 50 Years, Astron. Soc. Pacific. Conf. Ser. Vol.60 C.Corbally, R.O.Gray, R.F. Garrison eds., 172

CRAMER, N.: 1999, Calibrations *for B-type stars in the Geneva photometric system*, review article, New AR 43, 343

CRAMER, N.:1984a, *Relations between U, B, V intrinsic colours and Geneva photometry for B-type stars. The effective temperature scales*, A&A 132, 283

CRAMER, N.:1984b, *Relations between the β index and Geneva Photometry. The B-type Stars*, A&A 141, 215

GARRISON, R.F., GRAY, R.O.: 1991, *The Late B-Type Stars: Refined Classification, Confrontation with Strömgren Photometry and the effects of Rotation*, in Precision Photometry: Astrophysics of the Galaxy, (A.G. Davis Philip et al., Eds.) L. Davis Press, Schenectady, 173

HOUK, N., COWLEY, A.P.: 1975, *University of Michigan Catalogue of two-dimensional Spectral Types for the HD Stars*, Vol. 1 et subsq. Univ. Of Michigan, Ann Arbor

JASCHEK, C., JASCHEK, M.: 1987, in *The Classification of Stars*, Cambridge University Press, 94

KÜNZLI, M., NORTH, P., KURUCZ, R.L., NICOLET, B.: 1997, *A calibration of Geneva photometry for B to G stars in terms of T_{eff}, log g and [M/H]*, A&AS 122, 51

KURUCZ, R.L.: 1993, *Kurucz CD-ROM 13, ATLAS9 stellar atmosphere program and 2 km/s grid*

SCHMIDT-KALER, TH.: 1982, *Physical parameters of the stars*, in Landolt Bornstein (New Series) IV/2b

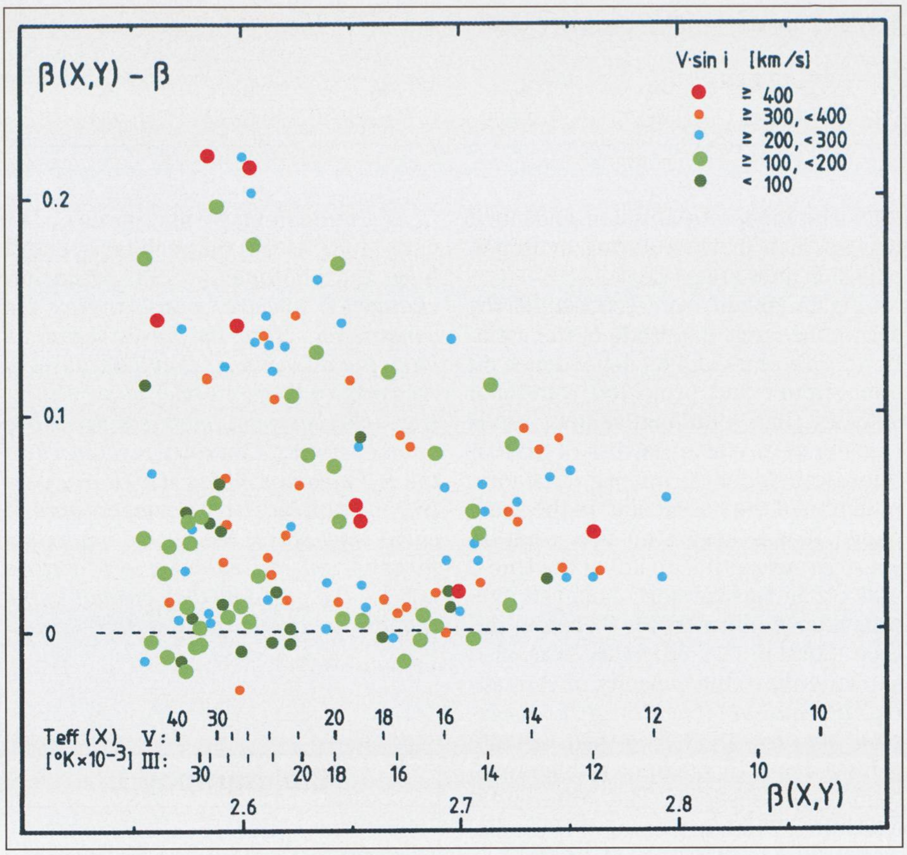

Fig. 45 The $\delta\beta = [\beta - \beta(X,Y)]$ «hyperindex» applied to Be stars. The latter are detected with great efficiency at the higher temperatures. Very fast rotators stand out conspicuously in that population. To be most effective regarding variability of the emission component, measurements should be carried out simultaneously in both systems. However, the $\beta(X,Y)$ estimate being practically insensitive to emission, knowledge of the epoch of the true β index measurement is most important. An estimate of the contribution of the emission feature's equivalent width in the H_β line is given by $\delta W \cong 34\,\delta\beta$ in Å units. Note also the apparent dependence of maximum emission on temperature (Figure taken from CRAMER, 1984b).

cally small $W(\beta)$, or a dwarf with a central emission in $H\beta$ simulating a small $W(\beta)$. This is clearly a case for the spectroscopists.» The author is undoubtedly right in most cases. But, had he read the (1984b) paper discussed above, he would most certainly have chosen a different example...

The next section of this article will continue the discussion of calibrations, but in the cases where interstellar extinction significantly affects the primary data and has to be accounted for.

NOËL CRAMER
Observatoire de Genève
CH-1290 Sauverny